A Markov Chain Channel Model for Active Transport Molecular Communication

Nariman Farsad, *Student Member, IEEE,* Andrew W. Eckford, *Member, IEEE,* and Satoshi Hiyama, *Member, IEEE,*

Abstract

In molecular communication small particles such as molecules are used to convey information. These particles are released by a transmitter into a fluidic environment, where they propagate freely (e.g. through diffusion) or through externals means (e.g. different types of active transport) until they arrive at the receiver. Although there are a number of different mathematical models for the diffusion-based molecular communication, active transport molecular communication (ATMC) lacks the necessary theoretical framework. Previous works had to rely almost entirely on full Monte Carlo simulations of these systems. However, full simulations can be time consuming because of the computational complexities involved. In this work, a Markov channel model has been presented, which could be used to reduce the amount of simulations necessary for studying ATMC without sacrificing accuracy. Moreover, a mathematical formula for calculating the transition probabilities in the Markov chain model is derived to complete our analytical framework. Comparing our proposed models with full simulations, it is shown that these models can be used to calculate parameters such channel capacity accurately in a timely manner.

Index Terms

Molecular Communication, Biological Information Theory, Mathematical Model, Markov Processes, Channel Capacity.

Nariman Farsad and Andrew W. Eckford are with the Department of Computer Science and Engineering, York University, 4700 Keele Street, Toronto, Ontario, Canada M3J 1P3. Emails: nariman@cse.yorku.ca, aeckford@yorku.ca

Satoshi Hiyama is with Research Laboratories, NTT DOCOMO Inc., Yokosuka, Kanagawa, Japan. Emails: hiyama@nttdocomo.co.jp

I. Introduction

Advancements in the field of nanotechnology are leading to *micro- or nano-scale devices*, typically performing only very simple and specific tasks due to limitations imposed by their small size [1]. This rapid progress is motivated by many potential applications such as: targeted drug delivery [2], nanorobotics [3], lab-on-chip devices [4], and point-of-care diagnostic chips [5]. In most of these applications communication between different components in each device, or between a biological entity and a component in the device, such as a nanosensor, is required. Therefore, one of the obstacles that must be overcome before many of these applications can be fully realized is devising a communication system for small scales [6], [7].

Conventional communication systems rely entirely on electronic or electromagnetic signals, and are typically used to carry information over distances ranging from a few centimetres (in Bluetooth technology) to millions of kilometres (for space communication). However, shrinking the current technology to very small dimensions (in the order of a few micrometers or even a few nanometres) is not a simple task. For example, shrinking the size of a transceiver antenna to nano-scales is difficult because the length of the antenna must be proportional to the wavelength of the carrier signal. To overcome this issue two different techniques have been proposed: electronic or electromagnetic communication with the help of novel materials such as carbon nanotubes [8], or *molecular communication* [9], [10].

In molecular communication small particles such as molecules are used to convey information. Information can be conveyed through encoding messages into the release timing [11], number [12], [13], concentration [14], or type of particles [15], which are released by a transmitter and propagate to a receiver. Two different propagation schemes can be employed: passive transport, and active transport. In passive transport, the information carrying particles propagate from the transmitter to the receiver by diffusing in the microfluidic medium without using external energy. In *active transport molecular communication* (ATMC), information carrying particles are transported by external means such as molecular motors or an external device such as a syringe pump. In [13], it was shown that active transport can achieve better information transmission rates over larger separation between the transmitter and the receiver. Therefore, in this work we consider active transport propagation scheme.

One of the biggest issues in designing and engineering molecular communication systems is

the lack of theoretical framework [16]. The theory of communication, which has been devised by communication engineers over the past century can not be applied directly to molecular communication. In the traditional communication paradigm, communication channels are always corrupted by noise. For example, thermal noise is always present in electronic devices. This noise introduces randomness into the communication channel. In molecular communication, the noise stems from the random nature of the propagation mechanism, which introduces uncertainty into the channel. Moreover, in confined channels analytical expression for this random propagation do not exist and are very difficult to derive, especially for ATMC.

A number of previous works have considered modeling the molecular communication channels. Most works focus on passive transport propagation schemes. Notable works in this direction include a general formulation of molecular communication as a timing channel under Brownian motion [17], [18], development of mathematical channel models for continuous diffusion [19], [20], introduction of binary concentration-encoded molecular communication [14], derivation of deterministic capacity expression for point-to-point, broadcast, and multiple-access molecular channels [21], capacity of molecular relay channels [22], closed-form expression for free diffusion propagation [23], modeling the noise in diffusion-based molecular communication [24], [25], stochastic model for channels with absorption, duplication and spontaneous emission phenomena [26], and modulation techniques using isomers as messenger molecules via diffusion [27].

Notable works concerning molecular motor based ATMC includes an analysis of information transfer rates using molecular motors [11], [28], a simple mathematical transport model for active transport propagation [29], optimization of the transmission zone and vesicular encapsulation [12], and design and optimization of the channel [30]–[32]. Finally, in [13], [33], [34], achievable information rates are compared under different propagation schemes. It is shown that active transport can achieve better information transmission rates.

Most previous works on ATMC rely on computer simulations to calculate quantities such as channel capacity. This follows because of the complex randomness associated with the propagation in confined spaces, which makes derivation of closed-form expressions difficult, especially when active transport propagation is used. The computer simulations can be time consuming, and could take days before simulation results could be obtained. Typically the computational complexities of these simulations increase as the size of the channel, or the number of information particles increase. Moreover, as the simulations become more realistic, the

computational complexities increase quickly. Therefore, solving complex design and optimization problems become time-consuming, tedious, and in some cases impossible. To remedy this problem, computationally efficient simulations and mathematical models are needed.

In this work we consider active transport propagation scheme where microtubule (MT) filaments moving over stationary kinesin [35], [36] are used to transfer the information particles from the transmitter to the receiver. We derive a Markov chain channel model for this propagation scheme, which reduces the amount of simulations required for characterizing the channel. Our contributions are as follows:

- Since ATMC channels with multiple MTs are very difficult to model due to dependencies between each MT, we first derive a Markov chain model for ATMC channel with a single MT. Although the same authors presented a simple mathematical channel model for ATMC with a single MT in [29], which was used to optimize the shape of the transmission zone, the new Markov chain model is much more accurate. For example, the model in [29] does not capture the effect that an MT can load multiple particles, whereas the new Markov chain model captures this effect.
- In practice, ATMC channels contain multiple MTs. Therefore, a Markov chain model for ATMC channels with multiple MTs is derived for reducing the amount of computational power required for calculating different channel parameters such as channel capacity.
- The Markov chain models for both single and multi-MT channels significantly reduce the simulation times required for characterizing the channel. The reduction in simulation times helps in solving design and engineering problems such as finding the shape of the optimal channel.
- The presented models are expandable and more realistic assumptions can be incorporated in these Markov chain models in the future.

The Markov chain models presented in this work can be considered as an *analytical toolbox*, and help in designing ATMC systems. Moreover, the new models provide new insights about ATMC channels, and can be potentially extended to other propagation schemes.

The rest of this paper is organized as follows. In Section II, an overview of the ATMC employing stationary kinesin and moving MT filaments is considered. In Section III a general information transmission model for this class of molecular communication systems is presented. In Section IV we derive our new Markov chain channel models, which can be used to characterize

the channel in a computationally efficient manner. The results comparing our newly proposed Markov chain models and full simulations used in previous works are presented in Section V. Finally, we present our concluding remarks and future works in Section VI.

II. Active Transport Molecular Communication

In this work we consider active transport propagation scheme, similar to the ones in [33]–[35], where MT filaments gliding over a kinesin-covered substrate are used to transfer the information particles from a transmitter to a receiver. In cells, MTs act as railways and kinesin is a molecular motor that acts as a locomotive carrying cargo from one location in the cell to another location by practically "walking" over the MT cytoskeleton structure that covers the inside of the cell. Each kinesin step is powered by hydrolysis of one molecule of adenosine triphosphate (ATP).

In [37], it was demonstrated that stationary kinesin can be used for MT filament motility. Moreover, in [35] it was demonstrated that using kinesin covered substrates and gliding MT filaments, which can be chemically prepared with relative ease, vesicles can be transported from one location to another. This makes ATMC using stationary kinesin (attached to a substrate) with gliding MT filaments on top very attractive for on-chip molecular communication [38]. We define the *microchannel* as a kinesin covered substrate, where the MTs can glide over the kinesin, and transport information particles from one location to another. Because the MT filaments glide right over the kinesin, the microchannel can be modelled as a 2-D environment viewed from the top. In this paper we assume that the shape of the microchannel can be rectangular, or a regular convex polygon viewed from the top. Regular convex polygons are equiangular (all angles are equal in measure) and equilateral (all sides have the same length). This class of polygons includes geometric shapes, ranging from an equilateral triangle, square, pentagon, and hexagon, all the way up to a circle as number of sides approaches infinity.

Although mathematical channel models we derive do not depend on the shape of the channel, we verify our models using these shapes only; partly because in [31], [32] we show that square and circular shaped channels are optimal for this type of active transport.

A. Modeling the Microtubule Motility

MT motion is random, and a closed-form expression for the movement of MT in confined space does not exist. Therefore, to study molecular communication systems based on this propagation

scheme, Monte-Carlo techniques proposed in [39] must be used to simulate the motion of the MT. In [40] it was shown that when an MT collides with the walls of the channel, it can glide along the channel walls. Moreover, when there are multiple MTs in the channel we can assume that the MTs do not collide with each other, and simply pass along each other. This is a valid assumption based on experimental observations in [36], and follows since the width of the MT filaments are only tens of nanometers thick.

Recall that the MTs move only in the x–y directions, and do not move in the z direction (along the height of the channel). Then motion of the MT can be modelled by discretizing time in to intervals of $\Delta\tau$ seconds. Given some initial position (x_0, y_0) at time $t = 0$, for any integer $k > 0$, the motion of the MT is given by the sequence of coordinates (x_i, y_i) for $i = 1, 2, \ldots, k$. Each coordinate (x_i, y_i) represents the position of the MT's head at the end of the time $t = i\Delta\tau$, and it is related to the position of the MT at the previous time step by

$$x_i = x_{i-1} + \Delta r \cos\theta_i, \tag{1}$$

$$y_i = y_{i-1} + \Delta r \sin\theta_i, \tag{2}$$

where Δr is the step size represented as an iid Gaussian random variable with mean and variance

$$E[\Delta r] = v_{\text{avg}}\Delta\tau, \tag{3}$$

$$\text{Var}[\Delta r] = 2D\Delta\tau, \tag{4}$$

with the v_{avg} being the average velocity of the MT, and D being the MT's diffusion coefficient. The angle θ_i is no longer independent from step to step: instead, for some step-to-step angular change $\Delta\theta$, we have that

$$\theta_i = \Delta\theta + \theta_{i-1}. \tag{5}$$

Now, for each step, $\Delta\theta$ is an iid Gaussian-distributed random variable with mean and variance

$$E[\Delta\theta] = 0, \tag{6}$$

$$\text{Var}[\Delta\theta] = \frac{v_{\text{avg}}\Delta\tau}{L_p}, \tag{7}$$

where L_p is the persistence length of the MT's trajectory. Using this model, the motion of the MT over a time period T can be simulated using Monte Carlo method. This model is the basis of all Monte Carlo simulations used in this work.

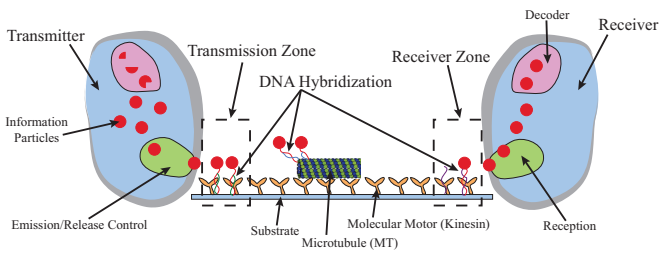

Fig. 1: Depiction of the communication environment [12].

B. ATMC Channel

Regardless of the shape of the microchannel, an area of the channel is designated as the *transmission zone* (where the transmitted particles originate), and an area is designated as the *receiver zone* (where the transmitted particles are destined). After information particles are released by the transmitter, they are assumed to be anchored to the transmission zone through deoxyribonucleic acid (DNA) hybridization bonds. The particles remain anchored until DNA covered MT filaments, moving over molecular motor tracks that cover the whole environment, load them through DNA hybridization bonds. For the loading to take place, an MT must pass close to the anchored particles. The loaded particles are then unloaded when the MT reaches the receiver zone. Again DNA hybridization is used for the unloading process. In [35], [36], the feasibility of the anchoring, loading, transportation, and the unloading process is demonstrated using laboratory experiments. This process is summarized in Figure 1.

Because studying ATMC channels using laboratory experimentation can be very laborious and time consuming, computer simulation have been used in previous works [10]. To simulate this channel, along with its corresponding loading process, the grid loading mechanism proposed in [12] is employed. In this scheme the transmission zone is divided into a square grid, where the length of each square in the grid is the same as the diameter of the information particles. These particles are then assumed to be randomly and uniformly distributed among the squares in the grid. In general, it is assumed that the MTs can load multiple particles, and the number of particles an MT can load is related to its length, which we know to be possible based on lab experiments [36]. This follows because after a maximum number of particles are loaded, there will be no more room available along the length of the MT for any other information particles.

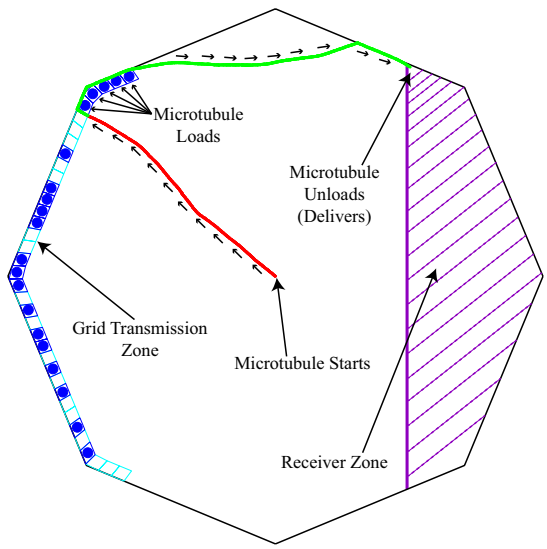

Fig. 2: Depiction of the simulation environment (i.e. ATMC channel viewed from the top). The squares along the wall of the channel on the left represent the transmission zone. The squares with a circle inside represent the grid locations where there is an anchored information particle.

Thus, if an MT enters a square which is occupied by a particle, and it has an empty loading slot available, it loads that particle. In our simulations we assume the size of the information particles is 1 μm, the length of the MTs is 10 μm and the maximum number of particles an MT can load is 5. We select these parameters based on laboratory experiments. For unloading, it is assumed that all the loaded particles are unloaded as soon as an MT enters the receiver zone.

Figure 2 shows this simulation environment, where an MT starts from the center of an octagon-shaped channel (8-sided regular polygon), and moves to the grid transmission structure on the left. The grid transmission zone is along the left walls of the channel and it is represented by all the squares. The squares with a circle inside represent the grid locations where there is an anchored information particle. In [13] it was shown that the optimal design for the transmission zone is along the walls of the channel. Therefore, in this work we always assume that the transmission zone is along the left walls of the channel, and the receiver zone is on the right side of the channel. As the MT enter the transmission zone, it picks up five information particles (in the figure, the color of the MT trajectory turns green after the first particle is loaded), and continues its path to the right until the picked up particles are unloaded at the receiver zone.

III. Information Transmission Model for ATMC

In molecular communication, messages can be encoded into information carrying particles using different schemes. For example, information can be encoded into the number, concentration, or type of the particles released. Regardless of the encoding scheme, information is transmitted through mass transfer (i.e. transfer of particles). In this work, we are not concerned with the encoding scheme used and instead we consider a general mass transfer model. We then derive a Markov chain channel model for ATMC based on this general framework, which is independent of the encoding scheme. Later in the Results section, to verify the performance of our models, we assume that the information is encoded in the number of information particles transmitted.

A predefined amount of time T representing the time duration for a single message transmission session is defined as *time per channel use* (TPCU). Given this time limit, the transmitted message might not be perfectly conveyed to the receiver because particles are delivered by MTs and they follow a random motion. It is possible that some of the particles will not arrive at the receiver after T has elapsed and therefore there is some information loss. This effect is similar in nature to the noise introduced by conventional electronic or electromagnetic channels.

Let $\mathcal{X} = \{0, 1, 2, \cdots, x_{max}\}$ be the set of possible particles that could be released by the transmitter, where x_{max} is the maximum number of particles the transmitter can release per channel use. Let $X \in \mathcal{X}$ be the number of information particles released into the medium by the transmitter, and let $Y(T) \in \mathcal{X}$ represent the number that arrive at the destination after TPCU duration T. At the receiver, X is a discrete random variable given by probability mass function (PMF) $P(x)$. Similarly, given X particles were released by the transmitter, and the TPCU duration T, $Y(T)$ is a discrete random variable given by conditional PMF $P(y(T) \mid x)$.

This conditional PMF is very important, and characterizes the ATMC channel. For example, it can be used to calculate parameters such as *channel capacity* [41], the maximum rate at which any communication system can *reliably transmit information* over a noisy channel. However, finding the PMF $P(y(T) \mid x)$ is non-trivial because the shape and the geometry of the molecular communication channels, plus the complex random motion of the MTs, generally rule out closed-form solutions. To overcome this issue, in previous works this PMF was estimated using Monte Carlo simulations presented in Algorithm 1. However, these simulations tend to be time consuming: the running time of Algorithm 1 is $O(L\frac{T}{\Delta\tau}Nx_{max}Q)$, where Q is the number of MTs

present in the channel being simulated, and L computational complexity overhead of simulating the loading and the unloading processes (line 7 of the algorithm). In this work we present a set of Markov chain models that can be used to calculate this PMF in a computationally efficient manner.

Algorithm 1 Monte Carlo simulation algorithm for calculating $P(y(T) \mid x)$.

1: **for** each value of $x \in \mathcal{X}$ **do**
2: **for** 1 to number of Monte Carlo trials N **do**
3: $t \leftarrow 0$
4: distribute information particles randomly in the grid transmission zone, and randomly select the starting location and the direction of motion of the MT(s).
5: **while** $t \leq T$ **do**
6: simulate the MT(s) motion in the channel for time step of $\Delta\tau$ seconds using Equations (1-2)
7: check and perform the loading and the unloading operations if necessary
8: $t \leftarrow t + \Delta\tau$
9: **end while**
10: save the obtained results for the current Monte Carlo trial
11: **end for**
12: **end for**

IV. Markov Chain Model of ATMC Channels

Deriving a channel model for ATMC with stationary kinesin and a single moving MT filament is very difficult because of the complex motion of the MT and the shape of the channel. Moreover, for ATMC channels with multiple MTs the problem becomes even more difficult because of the dependencies between all the MTs. In this case, although the movement of the MTs themselves can safely be considered to be independent [35], [40], the delivery of an information particle depends on whether it has already been picked up by other MTs. Therefore, many dependencies will be introduced into the system, which makes the derivation of mathematical models extremely difficult. To overcome these issues, we derive our channel models in two steps. We first consider

the case where a single MT is inside the channel. Although the problem of modeling the channel with a single MT is still quite complex, by focusing on a single MT, the dependencies between different MTs is eliminated and channel models that resemble closed-form expressions can be derived. We then extend the results to channels with multiple MTs and propose a Markov chain model, where transition probabilities can be calculated using simpler simulations compared to full simulations of the ATMC channels used in the past.

A. Modeling ATMC Using a Single MT

For the rest of this section we assume there is a single MT inside the channel, delivering the information particles. Therefore, an arbitrary information particle is received at the destination if it is picked up by this MT filament from the transmission zone, and then delivered to the receiver zone. Considering this fact, we define a *single MT trip* as the movement of the MT from anywhere in the channel to the transmission zone and then the receiver zone. For example, a single MT trip is shown in Figure 2. After the MT completes its first trip, subsequent trips are defined as the movement of the MT from the receiver zone to the transmission zone and back. During any trip, an MT can deliver zero or more information particles, up to its maximum load capacity.

Let $K(T)$ be the total number of MT trips during the TPCU duration T, and l_{max} be the maximum load capacity of the MT. Since the motion of the MT filament is random in nature, for a given value of TPCU T, the number of trips is random and represented by the probability mass function (PMF) $P(k(T))$. Therefore, the PMF $P(y(T) \mid x)$ can be written as

$$P(y(T) \mid x) = \sum_{k(T) \in K} P(y \mid x, k(T)) P(k(T)). \tag{8}$$

This follows because the number of particles that arrive at the destination during TPCU duration T $Y(T)$ depends on the number of trips the MT takes during the same TPCU duration $K(T)$.

From Equation (8) we can calculate $P(y(T) \mid x)$ if the PMFs $P(k(T))$ and $P(y \mid x, k(T))$ are known. The first PMF $P(k(T))$ can be estimated using a simple Monte Carlo simulation of the motion of the MT inside the channel. This Monte Carlo simulation is very simple compared to the full simulations used in previous works [12], [13], because it does not include simulation of the loading and unloading processes (lines 1, 4, 7, and 12 in Algorithm 1). Therefore, the

computational complexity of calculating PMFs $P(k(T))$ is $O(\frac{T}{\Delta\tau}N)$. To estimate the PMF $P(y \mid x, k(T))$, we derive a Markov chain model.

Let X_i be the number of information particles at the transmission zone at the *end* of the ith MT trip, Y_i be the total number of information particles already delivered to the receiver at the *end* of the ith MT trip, and D_i be the number of information particles delivered during the ith MT trip, for $i = 1, 2, 3, \ldots$. Therefore, $D_i \in \{0, 1, 2, \cdots, l_{max}\}$ is a random variable representing the number of particles delivered during the ith trip, where l_{max} is the maximum load the MT could have. Each trip is related to the next trip by the following properties

$$\begin{aligned} X_i &= X_{i-1} - D_i, \\ Y_i &= Y_{i-1} + D_i, \end{aligned} \tag{9}$$

where we assume $X_0 = X$ is the number of particles released by the transmitter at the beginning of the communication session, and $Y_0 = 0$ is the number of particles initially at the receiver.

We assume the number of information particles at the transmission zone and the receiver zone at the end of each trip iteration depends only on the previous iteration. Mathematically we have

$$P(Y_i \mid X, Y_{i-1}) = P(Y_i \mid X, Y_{i-1}, Y_{i-2}, \cdots, Y_0), \tag{10}$$

which satisfies the Markov property. Therefore, given the number of information particles released by the transmitter X, Y_is form a Markov Chain.

Figure 3 shows the graphical representation of this Markov chain. Each state represents the number of information particles delivered to the receiver with state s indicating the starting state. The transition probabilities can be calculated from the PMF $P(D_i|X_{i-1})$, the probability of the number of particles delivered during the ith trip given there were X_{i-1} particles at the transmission zone at the beginning of the trip, as follows

$$\begin{aligned} &P(Y_i = y_i \mid X = x, Y_{i-1} = y_{i-1}) = \\ &\begin{cases} P(D_i = y_i - y_{i-1} | X_{i-1} = x - y_{i-1}) & y_{i-1} \leq y_i \leq y_{i-1} + l_{max}. \\ 0 & \text{otherwise} \end{cases} \end{aligned} \tag{11}$$

For the first trip, the MT can start from anywhere in the channel uniformly at random. However for all the subsequent trips, the MT starts from the receiver zone. Therefore, to distinguish

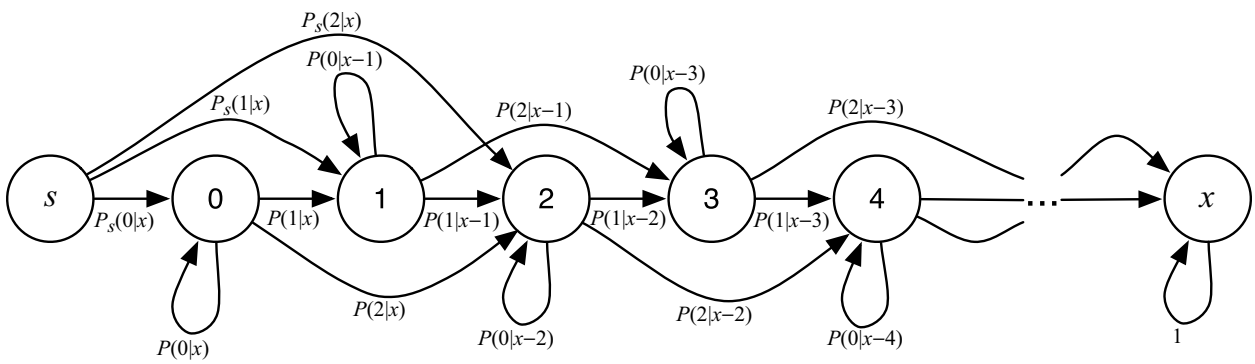

Fig. 3: The Markov chain representing the number of information particles received at the destination. State s is the starting state, and each of the other states represents the number of information particles that are delivered to the destination. We assume the maximum number of particles a single MT can load is $l_{max} = 2$ to generate a simplified and comprehensible figure. It is assumed that x information particles are released by the transmitter. The transition probabilities are given by $P(D_i = d \mid X_{i-1} = x_{i-1})$. The transition probabilities are different for the starting state s, since for the first trip the MT can start its trip from anywhere in the channel, while for subsequent trips the MT starts from the receiver.

between these two cases, we use the notation $P_s(D_1|X_0)$ for the first trip, and $P(D_j|X_{j-1})$, with $j = 2, 3, \ldots$, for all the subsequent trips. Moreover, we assume

$$\begin{aligned} P(D_2 = d|X_1 = x) =& P(D_3 = d|X_2 = x) = \cdots \\ &= P(D_i = d|X_{i-1} = x) = \cdots . \end{aligned} \tag{12}$$

This assumption is valid since the number of information particles delivered at trip iterations greater than one, are dependent only on the number of information particles in the transmission zone at the end of the previous iteration. The equality follows because after the first trip, each subsequent trip starts from the receiver zone.

We define the probability transition matrix given x particles are released by the transmitter as $\mathbf{P}(x)$. Equation (13) shows this $(x+2) \times (x+2)$ probability transition matrix. Each element in the matrix is equal to 0, $P_s(D_1|X_0)$, or $P(D_j|X_{j-1})$. The PMFs $P_s(D_1|X_0)$ and $P(D_j|X_{j-1})$ can be estimated from Monte Carlo simulations that are much more efficient than the full simulation used in [12], [13]. Instead of simulating multiple MT trips, only single trip simulations are needed

$$\mathbf{P}(x) = \begin{bmatrix} 0 & P_s(0|x) & P_s(1|x) & P_s(2|x) & \cdots & P_s(l_{max}|x) & 0 & 0 & 0 & \cdots \\ 0 & P(0|x) & P(1|x) & P(2|x) & \cdots & P(l_{max}|x) & 0 & 0 & 0 & \cdots \\ 0 & 0 & P(0|x-1) & P(1|x-1) & \cdots & P(l_{max}|x-1) & 0 & 0 & 0 & \cdots \\ 0 & 0 & 0 & P(0|x-2) & \cdots & P(l_{max}|x-2) & 0 & 0 & 0 & \cdots \\ \ddots & \ddots & \ddots & \ddots & \ddots & \ddots & \ddots & \ddots & \ddots & \ddots \\ \cdots & 0 & 0 & 0 & 0 & 0 & 0 & P(0|2) & P(1|2) & P(2|2) \\ \cdots & 0 & 0 & 0 & 0 & 0 & 0 & 0 & P(0|1) & P(1|1) \\ \cdots & 0 & 0 & 0 & 0 & 0 & 0 & 0 & 0 & 1 \end{bmatrix} \tag{13}$$

for estimation of $P_s(D_1|X_0)$ and $P(D_j|X_{j-1})$. Therefore in Algorithm 1, instead of using the TPCU interval T in line 5 we use the time for a single MT trip T_{1trip} which is typically much smaller than T. The running time of these simulations is therefore given by $O(L\frac{T_{\text{1trip}}}{\Delta\tau}Nx_{max})$.

In Equation (8), we showed that when PMFs $P(k(T))$ and $P(y \mid x, k(T))$ are known, the PMF $P(y(T) \mid x)$ can be calculated. The PMF $P(k(T))$ can be estimated using a simple Monte Carlo simulation, while the PMF $P(y \mid x, k(T))$ can be calculated using the probability transition matrix $\mathbf{P}(x)$ as

$$P(y \mid x, k(T)) = \mathbf{s}(x)\mathbf{P}(x)^{k(T)}, \tag{14}$$

where $\mathbf{s}(x)$ is the initial state distributions represented as a row vector by

$$\mathbf{s}(x) = (1, \underbrace{0, 0, \ldots, 0}_{x+1}). \tag{15}$$

This follows because we always assume that the Markov chain starts at state s. Substituting Equation (14) into Equation (8), we have

$$P(y(T) \mid x) = \sum_{k(T)\in K} P(k(T))\mathbf{s}(x)\mathbf{P}(x)^{k(T)}. \tag{16}$$

Therefore, the PMF $P(y(T) \mid x)$ can be estimated if $P(k(T))$, $P_s(D_1|X_0)$ and $P(D_j|X_{j-1})$ are known. All these three PMFs can be estimated using simple Monte Carlo simulations, where their combined computational time would be $O(\frac{T}{\Delta\tau}N + L\frac{T_{\text{1trip}}}{\Delta\tau}Nx_{max})$, which is less than that of the full simulations used in previous works.

To further reduce the simulation time required for calculating the PMF $P(y(T) \mid x)$, we derive an estimated mathematical expression for the transition probabilities. For simplicity, we assume both PMFs $P_s(D_1|X_0)$ and $P(D_j|X_{j-1})$ are the same (i.e. there is no difference between the first initial trip or any subsequent trips). Therefore, for this case the state s in Figure 3 is removed and the transition probability matrix becomes a $(x+1) \times (x+1)$ matrix. The initial state is also changed to state 0 with probability one. To derive our model, we also assume a grid loading structure is used to capture the loading process with n squares in the grid, where $n \geq x_{max}$ represents the number of places (squares) where an information particle could be released from. Moreover, a single information particle can be placed inside each square until it is picked up by an MT. In [13], it was shown that the optimal transmission area is along the walls of the channel. Therefore, in this work we also assume that the transmission zone is always along the walls of the channel.

Let p_{D_i} be the probability that an information particle from any of the squares is delivered to the destination during the ith MT trip. We can calculate this probability as

$$p_{D_i} = p_V \times \frac{x_{i-1}}{n}, \tag{17}$$

where x_{i-1} is the number of information particles in the transmission zone at the end of the previous trip, and p_V is the probability that a square in the grid is visited during a single MT trip. For simplicity, we assume that this probability is the same for all the squares in the grid. The same Monte Carlo simulation which is used to estimate $P(k(T))$, can be used to estimate p_V through saving an extra parameter. Therefore, the computational complexity of calculating $P(k(T))$ and p_V together is $O(\frac{T}{\Delta\tau}N)$.

The PMF $P(D_i|X_{i-1})$ can be estimated from p_{D_i} as

$$P(D_i = d \mid X_{i-1} = x_{i-1}) = \begin{cases} \binom{n}{d} p_{D_i}^d (1-p_{D_i})^{n-d} & 0 \leq d \leq l_{max} - 1 \\ \sum_{m=l_{max}}^{n} \binom{n}{m} p_{D_i}^m (1-p_{D_i})^{n-m} & d = l_{max} \\ 0 & \text{otherwise} \end{cases}. \tag{18}$$

This follows since the probability that an information particle is delivered from a specific square in the grid is independent from other squares, and the maximum load an MT can have is l_{max}.

The PMF $P(y(T) \mid x)$ can be calculated using this technique with a computational complexity of $O(\frac{T}{\Delta\tau}N)$. This is significantly smaller than the computational complexity of full simulation $O(L\frac{T}{\Delta\tau}Nx_{max})$, which was used in previous works.

B. Modeling ATMC Using Multiple MTs

In the previous section, we derived a Markov chain model for ATMC systems employing a single MT. To do this we defined a single MT trip as the motion of the MT from the receiver zone to the transmission zone and back, and used a random variable $K(T)$ to represent the number of trips during the TPCU interval T. When there is only one MT in the channel, the trips are ordered (i.e. each trip happens after the previous trip) and therefore the Markov property of Equation (10) holds. However, if there are multiple MTs in the channel, two or more MTs might be visiting the transmission zone simultaneously or be in between trips. Therefore, the number of particles delivered at a given time interval depends on all the MTs and the Markov property of Equation (10) does not hold. Because of the interdependence of MTs and the fact that the Markov property does not hold, modeling ATMC when multiple MTs are inside the channel is extremely difficult. To overcome these issues, we discretize time instead of MT trips.

We discretize the TPCU value T into M equal time intervals of Δt as

$$T = M\Delta t. \tag{19}$$

Therefore, T is broken down into M time steps. Let $m = 1, 2, \ldots M$ be each of these time steps. Furthermore, let X_m be the number of information particles at the transmission zone at the *end* of the mth time step, Y_m be the total number of information particles already delivered to the receiver at the *end* of the mth time step, and D_m be the number of information particles delivered during the mth time step. Therefore, $D_m \in \{0, 1, 2, \cdots, X_{m-1}\}$ is a random variable representing the number of particles delivered during the mth time step of length Δt. Each time step is related to the next time step by the following properties

$$\begin{aligned} X_m &= X_{m-1} - D_m, \\ Y_m &= Y_{m-1} + D_m, \end{aligned} \tag{20}$$

where we assume $X_0 = X$ is the number of particles released by the transmitter at the beginning of the communication session, and $Y_0 = 0$ is the number of particles initially at the receiver.

With this new discretization we can derive a Markov chain model similar to the one we derived in the previous section for ATMC channels with a single MT. In this case the probability transition matrix given x particles are released by the transmitter is given by

$$\mathbf{P}(x) = \begin{bmatrix} P(0|x) & P(1|x) & P(2|x) & \cdots & P(x|x) \\ 0 & P(0|x-1) & P(1|x-1) & \cdots & P(x-1|x-1) \\ 0 & 0 & P(0|x-2) & \cdots & P(x-2|x-2) \\ \ddots & \ddots & \ddots & \ddots & \ddots \\ \cdots & 0 & P(0|2) & P(1|2) & P(2|2) \\ \cdots & 0 & 0 & P(0|1) & P(1|1) \\ \cdots & 0 & 0 & 0 & 1 \end{bmatrix} \tag{21}$$

where transition probabilities are in the form $P(D_m = d|X_{m-1} = x)$ for $d = 0, 1, 2, \cdots, X_{m-1}$. Because of the dependencies between multiple MTs discussed earlier, deriving a closed-form expression for the transition probabilities is not possible. However, the transition probabilities can be estimated using Monte Carlo simulations by using Δt instead of T in line 5 of Algorithm 1. The duration of these Monte Carlo simulations would be shorter than full simulations used in the past since the time step Δt is smaller than the TPCU value T. The computational complexity of these Monte Carlo simulation are $O(L\frac{\Delta t}{\Delta \tau}Nx_{max}Q)$. Therefore, in general we would expect M folds improvement in computation time of the simulations compared to full simulations of the ATMC channels. Moreover, we would expect the the estimated PMFs be more accurate for smaller M (i.e. larger time steps Δt) and less accurate for larger M (i.e. smaller time steps Δt). This is because smaller time steps capture the motion of the MTs for a shorter amount of time and therefore calculated transition probabilities would be less accurate. Similarly, larger time steps capture a longer duration of motion of the MTs, which results in more accurate estimation of transition probabilities.

V. Results and Discussions

We verify the accuracy of our proposed model with respect to the full computer simulation environment used in [12], [13]. To compare the PMFs obtained using our Markov chain models with the PMFs obtained using full Monte Carlo simulation, we use Kullback-Leibler (K-L) distance (also known as Kullback-Leibler divergence or relative entropy) [41]. K-L distance is calculated as

$$D\left(P_{\text{sim}} \parallel P_{\text{model}}\right) = \sum_{y(T)\in\mathcal{X}} P_{\text{sim}} \log \frac{P_{\text{sim}}}{P_{\text{model}}}, \tag{22}$$

where P_{sim} and P_{model} represent the PMF $P(y(T) \mid X = x)$, estimated using full Monte Carlo simulations or our Markov chain models, respectively. K-L distance signifies the amount of information lost if P_{model} is used instead of P_{sim}.

To better quantify this value, instead of using it directly we use the ratio of K-L distance over the entropy of the PMF $P_{\text{sim}}(y(T) \mid X = x)$, which is obtained through full Monte Carlo simulations. In this case the entropy is calculated as

$$H(Y(T)|X = x) = \\ - \sum_{y(T)\in\mathcal{X}} P_{\text{sim}}(y(T) \mid X = x) \log P_{\text{sim}}(y(T) \mid X = x), \tag{23}$$

and it signifies the average number of bits needed to represent the PMF. Using Equations (22) and (23) our performance measure is given by

$$\mathcal{R} = \frac{D\left(P_{\text{sim}} \parallel P_{\text{model}}\right)}{H(Y(T)|X = x)}. \tag{24}$$

This ratio gives a direct measure of normalized error for the estimation. In general the closer the ratio is to zero, the better our models estimate the PMFs. However, it is still difficult to decide what would be a good value for this ratio (i.e. for what ratio the Markov chain calculated PMFs are acceptable compared to full Monte Carlo simulations).

To further investigate the accuracy of our models, we calculate an actual channel parameter known as *channel capacity* using both full simulation based PMFs and Markov chain model based PMFs. For calculating the channel capacity, we assume that the information is encoded in the number of information particles transmitted. The channel capacity is calculated using PMF $P(y(T) \mid x)$ as

$$C = \max_{P(x)} I(X; Y(T)), \tag{25}$$

where $I(X; Y(T))$ is the mutual information between X and $Y(T)$, defined as

$$I(X; Y(T)) = E\left[\log_2 \frac{P(y(T) \mid x)}{\sum_x P(y(T) \mid x)P(x)}\right], \tag{26}$$

where $E[\cdot]$ represents expectation.

Mutual information can be calculated if the two PMFs $P(y(T) \mid x)$, and $P(x)$ are known. Channel capacity is the maximum mutual information over all possible PMFs $P(x)$. If $P(y(T) \mid x)$ is known, we can calculate mutual information for any $P(x)$. Moreover, the Blahut-Arimoto algorithm [42], [43] can be used to find the exact PMF $P(x)$ that maximizes the mutual

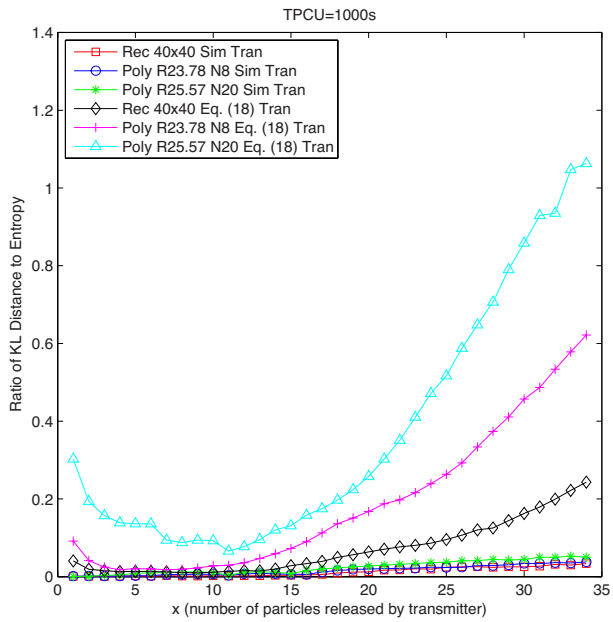

Fig. 4: The ratio of K-L distance between the simulation and model based PMFs to the entropy of simulation based PMFs for different values of x (the number of particles released by the transmitter). Channels contain only a single MT.

information. This follows because mutual information is convex with respect to $P(x)$ and Blahut-Arimoto algorithm performs convex optimization to find the exact maximum. Therefore, if PMF $P(y(T) \mid x)$ is known, we can calculate the channel capacity of the molecular communication system in a straightforward manner.

In the rest of this section, the parameters used in all Monte Carlo simulations are as follows: simulation time steps of $\Delta T = 0.1$ seconds (this is different from the discretization time step Δt introduced in the previous section), MT diffusion coefficient $D = 2.0 \cdot 10^{-3}$ µm^2/s, average speed of the MT $v_{\text{avg}} = 0.5$ µm/s, and persistence length of the MT trajectory $L_p = 111$ µm. We also assume the size of the information particles is 1µm, the average length of the MTs is 10µm, and each MT can load up to 5 information particles in one trip from the transmission zone to the receiver zone. These parameters are all selected based on experimental observations of DNA covered MTs moving over a kinesin covered substrate [35], [40].

A. ATMC Channels Using a Single MT

First, we consider the Markov chain model derived for the channels with a single MT. For this case, three different channels are considered: a square channel of 40 μm × 40 μm, an 8-sided regular polygon (octagon) channel with radius 23.78 μm, and a 20-sided regular polygon with radius 25.57 μm. The grid transmission zone structure is always assumed to be along the channel walls, which was shown to be the optimal design in [29].

We consider our Markov models for single MT channels, where the transition probabilities $P(D_i \mid X_{i-1})$ can be estimated using two different techniques: Monte Carlo simulations, and Equation (18). When Monte Carlo simulations are used to estimate the transition probabilities, two sets of simulations are performed to estimate $P_s(D_1 \mid X_0)$, the number of particles delivered during the first trip, and $P(D_j|X_{j-1})$, the number of particles delivered during subsequent trips ($j = 2, 3, \ldots$). When Equation (18) is used for calculation of transition probabilities, an estimate for p_v (the probability that a square in the grid loading structure is visited) is required. This probability can be obtained from the same simulation that is used to estimate the PMF of the number of MT trips $P(k(T))$.

Figure 4 shows the results for the TPCU value of $T = 1000$ seconds. The ratio of K-L distance between the simulation and model based PMFs to the entropy of simulation PMFs is plotted against different values of x (number of particles released by the transmitter). We use the term "Sim Tran" in the plot legend to indicate the case where the transition probabilities are calculated using Monte Carlo simulations, and the term "Eq. (18) Tran" to indicate the case where transition probabilities are calculated using Equation (18). In practice large number of information particles can be released by the transmitter. At the same time, channel capacity increases with the size of the symbol set. Therefore, the value of this ratio at $x_{max} = 34$ is considered. We can see that, as expected, when simulations are used to estimate the PMFs, lower ratio is achieved. However, transition probabilities and hence the PMFs can be estimated more quickly when Equation (18) is used.

Another property observed in Figure 4 is that for "Eq. (18) Tran" plots the $\mathcal{R}$ ratio increases as x_{max} increases. This follows because of some independence assumptions made in derivation of Equation (18), which simplifies the model. In particular, we have assumed that the probability that a particle is in a given square during the ith MT trip is x_{i-1}/n. However, this assumption

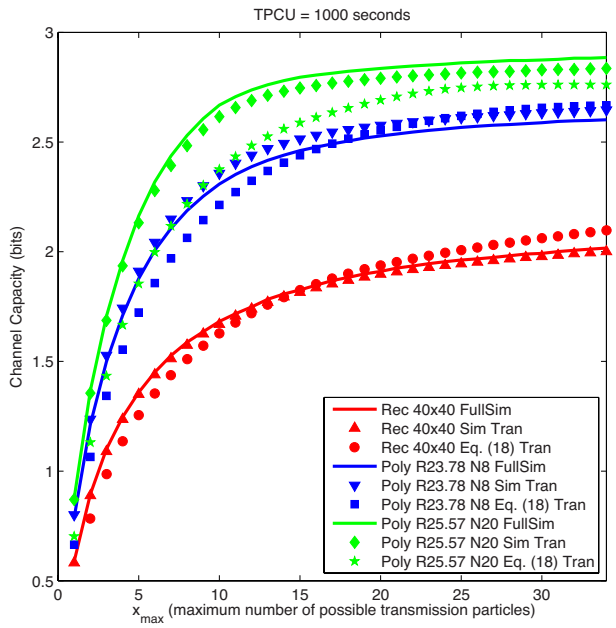

Fig. 5: Channel capacity in bits versus $x_{\max}$, maximum number of information particles that can be released by the transmitter, calculated based on full simulations (solid lines), and Markov chain models (points). Channels contain only a single MT.

does not take into consideration the fact that the particle may have already been picked up from this particular square. In other words, for each trip the remaining particles are redistributed across the squares. This error increases as the symbol size increases and hence the increasing $\mathcal{R}$ ratio.

To further investigate the estimated PMFs, and determine if they are accurate enough to characterize the channel, we use them to calculate the channel capacity, which is one of the most important parameters of any communication channel. In particular, we calculate the channel capacity based on the PMF $P(y(T) \mid x)$ obtained using three different methods: full Monte Carlo simulations, our Markov chain model with full simulation-based transition probabilities, and our Markov chain model with transition probabilities estimated using Equation (18).

Figure 5 shows the calculated channel capacities versus x_{max}, the maximum number of particles the transmitter can transmit. The solid lines represent the channel capacities calculated using full Monte Carlo simulations, while the point plots show the channel capacities calculated using our Markov chain models. From the figure we can see that when the Markov chain model

with simulation estimation of transition probabilities is used, the estimated channel capacities are very close to the ones obtained from full simulations. Although, the channel capacities calculated using our model with transition probabilities based on Equation (18) are not as accurate, they are still relatively close to the ones obtained using full simulations, and can be calculated much faster. Comparing Figures 4 and 5, we can see that although the estimated PMFs may not be extremely accurate, the estimated channel capacities are fairly accurate. Therefore, since we are modelling the molecular communication channel from a telecommunication perspective, our model's performance is satisfactory.

Finally, we compare the computer simulation times required for calculating the PMF $P(y(T) \mid x)$ based on three different cases: full simulation, Markov chain model based on simulation estimation of $P(k(T))$, $P_s(D_1 \mid X_0)$, and $P(D_j|X_{j-1})$, and Markov chain model based on simulation estimation of $P(k(T))$ and p_v and using Equation (18). All our Monte Carlo simulations use the same propagation engine for the motion of the MT inside the channel. Therefore, although each simulation estimates a different PMF, the propagation engine is the same between them. Therefore, the algorithm used for computing different PMFs are computationally very similar.

The simulation times are all obtained by running our simulation code on the same notebook: Mac Book Pro (mid 2010) with 2.66 GHz Intel Core i7, 8GB 1067MHz DDR3 RAM, and Mac OS X version 10.7.4. The simulations were written in Matlab [44] for Mac OS X. Figure 6 shows the resulting simulation times for calculating these PMFs, when TPCU value is $T = 2000$ seconds, the number of information particles that are released by the transmitter ranges from 1 to 34, and the number of iteration used for each of the Monte Carlo simulations is 5000.

When instead of full simulations, the Markov model is used with simulated transition probabilities the simulation times are reduced by more than half. Moreover, when Equation (18) is used to estimate the transition probabilities, the simulations duration is reduced by more than 25 times compared to full simulations. For example, for the 40×40 square channel the simulation durations are about 77 hours, 26 hours and 2 hours for the full simulation, Markov chain model with simulation estimation of transition probabilities, and Markov chain model with transition probabilities calculated using Equation (18), respectively. Although in the latter case the estimated PMF is not as accurate as the other two methods, the gains in terms of simulation time are significant compared to the loss in accuracy. From these results, we propose using Equation (18) and the Markov model for initial system design and optimization, and using

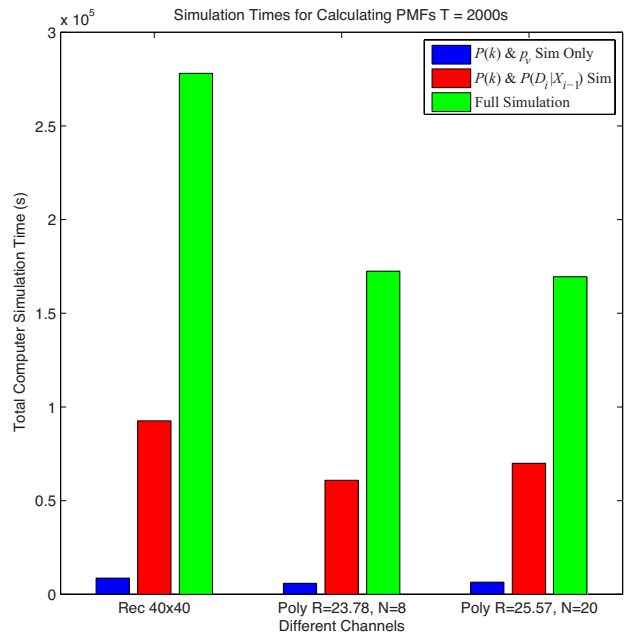

Fig. 6: The simulation times required to calculate the PMFs $P(y(T) \mid x)$ for $T = 2000$ s, $x = 1, 2, \ldots, 34$, and 5000 iteration per each Monte Carlo simulation.

simulation based calculation of transition probabilities for final stages of system design.

B. ATMC Channels Using Multiple MTs

In this section we consider the Markov chain channel model for ATMC using multiple MTs. We use the same three channels that were considered in the previous section. To get an accurate estimation of the transition probabilities, the discretization time steps Δt must be such that at least a single MT trip is captured in each time step for most of the MTs in the channel. Let P be the perimeter of the channel, and v_{avg} be the average speed of the MTs as defined earlier. Because MTs mostly follow the walls of the channel, the desirable values for Δt are given by

$$\Delta t \geq \frac{P}{v_{\text{avg}}}. \tag{27}$$

In general the larger the value of Δt is compared to the ratio on the right hand side of the equation, the better the transition probabilities are estimated. This follows because in this case more MT trips are captured in each time steps which results in a more accurate estimation of the transition probabilities of our Markov chain model.

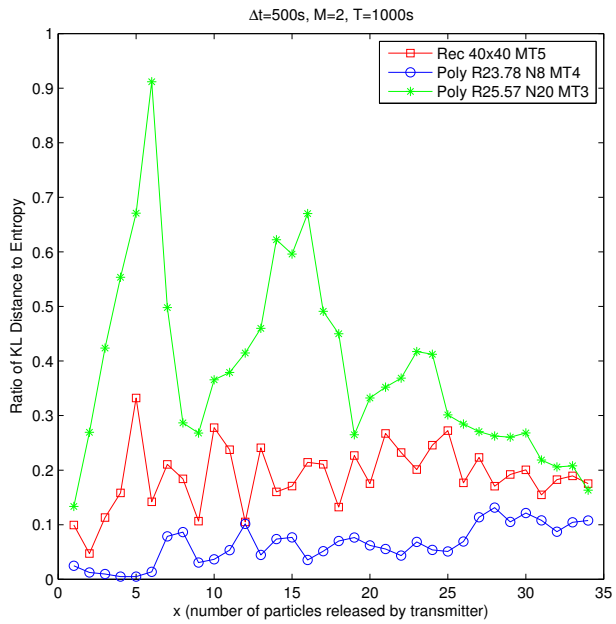

Fig. 7: The ratio of K-L distance between the simulation and model based PMFs to the entropy of simulation PMFs for different values of x (the number of particles released by the transmitter). Channels contain multiple MTs.

Figure 7 plots the ratio of K-L distance between the simulation and model based PMFs to the entropy of simulation PMFs for different values of x. We assume there are 5 MTs in the square channel, 4 MTs in the octagon channel, and 3 MTs in the 20-sided polygon channel. We have chosen different numbers to demonstrate that the model works for any number of MTs. For the channels considered in this plot we assume $\Delta t = 500$ seconds (this value satisfies Equation (27) criterion), and the TPCU is 1000 seconds (i.e. the number of steps $M = 2$).

In practice large number of information particles can be released by the transmitter. At the same time, channel capacity increases with the size of the symbol set. Therefore, the value of this ratio at $x_{\max} = 34$ is considered. For each channel the number of time steps is $M = 2$, and therefore the discretization intervals are one half the TPCU duration. Therefore, the transition probabilities can be calculated in one half the time it takes for full simulations.

To further investigate the accuracy of the estimated PMFs, we use them to calculate the channel capacity, which is one of the most important parameters of any communication channel. Figure 8 compares the channel capacity of each channel obtained through full simulations (lines plots),

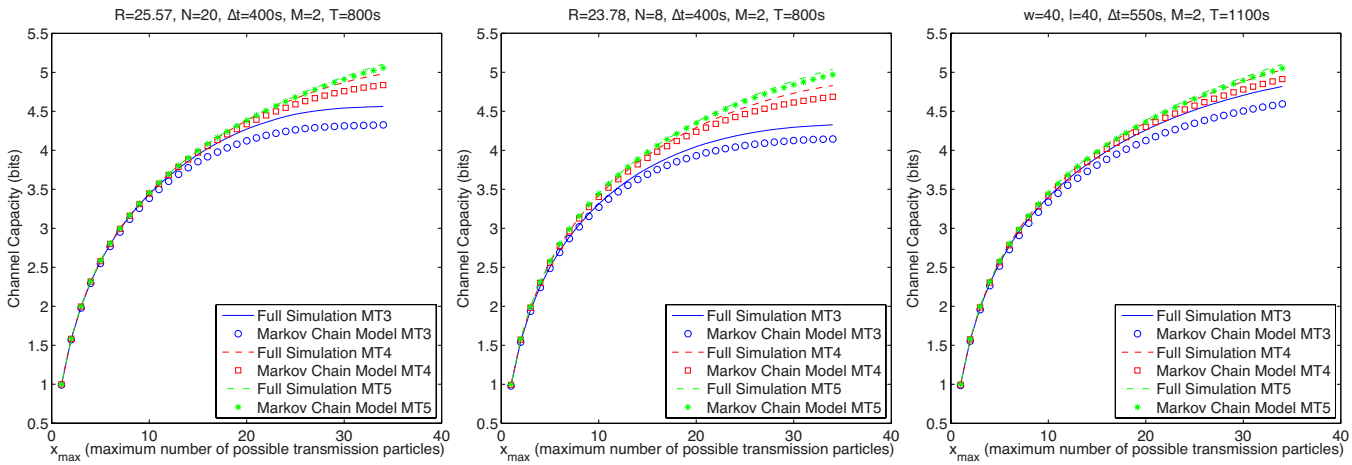

(a) (b) (c)

Fig. 8: Channel capacity in bits versus $x_{\max}$, maximum number of information particles that can be released by the transmitter, for both full simulations and Markov chain model for multiple MTs: (a) 20-sided regular polygon channel with radius of 25.57 μm, (b) octagon channel with radius of 23.78 μm, and (c) square channel of length 40 μm.

to the ones calculated using our proposed Markov chain model (point plots). For each channel, the number MTs are taken to be 3, 4, and 5. For both polygon channels $\Delta t = 400$ seconds and $T = 800$ seconds, and for the square channel $\Delta t = 550$ seconds and $T = 1100$ seconds. We chose these value since the plots for different number of MTs are all visible on a single plot at these durations, and to show that our model works for different values of T. As can be seen the channel capacities can be estimated fairly accurately at half the time it takes for full simulations. Moreover, by increasing the value of M (i.e. decreasing the discretization time intervals) channel capacities can be estimated more quickly at the cost of a loss in accuracy.

The PMFs $P(y(T) \mid x)$ estimated using our Markov chain model are fairly accurate and become more accurate as the time step durations Δt increases compared to the term on the right hand side of Equation (27). This effect can be seen in the figure; the octagon channel has a better estimated channel capacity, since it has a smaller perimeter compared to the 20-sided polygon channel for different number of MTs. Therefore, for $\Delta t = 400$ more MT trips are captured in estimated tradition probabilities of the Markov chain model, which results in a slightly more accurate estimation of channel capacity.

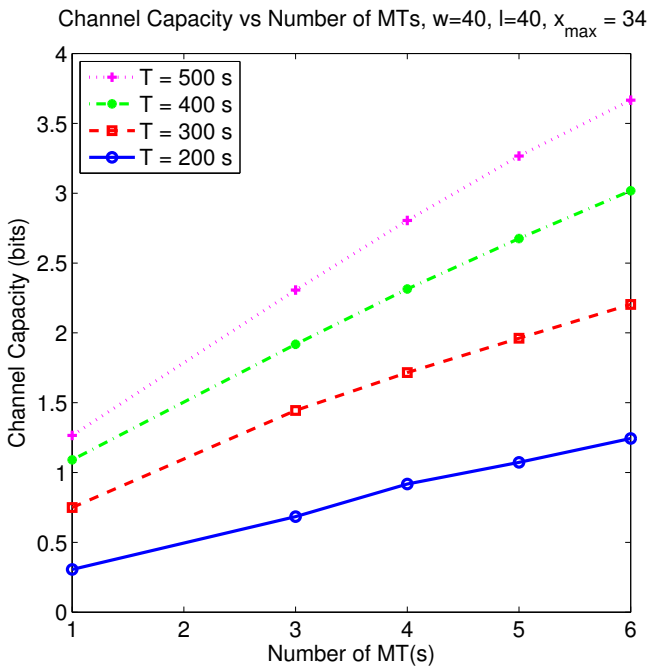

Fig. 9: Channel capacity in bits versus the number of MTs for a square channel with 40 μm sides and $x_{\max} = 34$. Capacity increases linearly with the number of MTs.

Finally, as can be seen channel capacity increases with the number of MTs for all channels. In Figure 9, the channel capacity is plotted for different number of MTs in the channel. The channel is a square channel with 40 μm sides, and the size of the message set is 34. As can be seen capacity increases linearly with number of MTs for each value of T.

VI. Conclusion and Future Work

In this paper we have considered active transport molecular communication (ATMC), where microtubule (MT) filaments moving over kinesin covered substrate are used as carriers of information particles from a transmitter to a receiver. We developed a set of Markov chain channel models which could be used to reduce the amount of simulations that are required for studying this class of molecular communication systems. We first considered single MT channels, and then developed a model for multi-MT channels. Finally, we compared the accuracy of the proposed Markov chain model with full Monte Carlo simulations used in previous works. Based on the obtained results we showed when our Markov chain model is used with simulation based

estimation of transition probabilities, the PMFs are estimated fairly accurately compared to full simulations, with less than half the amount of simulation time. Moreover, we showed when the presented mathematical formula is used to estimate the transition probabilities, there was a loss in accuracy compared to full simulation based method. However, the amount of necessary simulations dropped significantly by more than 25 times the case where full simulation was employed. Similarly, for the channels with multiple MT, we showed that the PMFs can be estimated using our Markov chain model fairly accurately at a fraction of the time of full simulations.

The derived Markov chain channel models have a number of benefits. First, because this type of ATMC is ideal for many on-chip applications, our models could be used as a mathematical framework to solve many different design, engineering, and optimization problems in a timely manner. Second, these models are much more accurate than our previous model [29], which was used as a tool for optimizing the shape of the transmission zone. Third, the proposed models can be considered as an *analytical toolbox* and can be potentially extended to other propagation schemes. Moreover, more realistic assumptions can be incorporated into the model in future works. Finally, the relation between the developed models in this paper and previously developed models such as equivalent queueing system with multiple servers merits investigation as part of future works.

REFERENCES

[1] A. Requicha, "Nanorobots, NEMS, and nanoassembly," *Proceedings of the IEEE*, vol. 91, pp. 1922–1933, nov 2003.

[2] O. Veiseh, J. W. Gunn, and M. Zhang, "Design and fabrication of magnetic nanoparticles for targeted drug delivery and imaging," *Advanced Drug Delivery Reviews*, vol. 62, no. 3, pp. 284–304, 2010.

[3] G. M. Patel, G. C. Patel, R. B. Patel, J. K. Patel, and M. Patel, "Nanorobot: A versatile tool in nanomedicine," *Journal of Drug Targeting*, vol. 14, no. 2, pp. 63–67, 2006.

[4] R. Daw and J. Finkelstein, "Insight: Lab on a chip," *Nature*, vol. 442, no. 7101, pp. 367–418, 2006.

[5] P. Yager, T. Edwards, E. Fu, K. Helton, K. Nelson, M. R. Tam, and B. H. Weigl, "Microfluidic diagnostic technologies for global public health," *Nature*, vol. 442, pp. 412–418, July 2006.

[6] I. F. Akyildiz, F. Brunetti, and C. Blazquez, "Nanonetworks: A new communication paradigm," *Computer Networks*, vol. 52, no. 12, pp. 2260–2279, 2008.

[7] S. F. Bush, *Nanoscale Communication Networks*. Artech House, 1 ed., 2010.

[8] K. Jensen, J. Weldon, H. Garcia, and A. Zettl, "Nanotube radio," *Nano Letters*, vol. 7, no. 11, pp. 3508–3511, 2007.

[9] S. Hiyama, Y. Moritani, T. Suda, R. Egashira, A. Enomoto, M. Moore, and T. Nakano, "Molecular communication," in *Proc. of 2005 NSTI Nanotechnology Conference*, pp. 391–394, 2005.

[10] T. Nakano, M. Moore, F. Wei, A. Vasilakos, and J. Shuai, "Molecular communication and networking: Opportunities and challenges," *IEEE Transactions on NanoBioscience*, vol. 11, pp. 135–148, june 2012.

[11] A. W. Eckford, "Timing information rates for active transport molecular communication," in *Nano-Net*, vol. 20 of *Lecture Notes of the Institute for Computer Sciences, Social Informatics and Telecommunications Engineering*, pp. 24–28, Springer Berlin Heidelberg, 2009.

[12] N. Farsad, A. W. Eckford, S. Hiyama, and Y. Moritani, "Quick system design of vesicle-based active transport molecular communication by using a simple transport model," *Nano Communication Networks*, vol. 2, no. 4, pp. 175–188, 2011.

[13] N. Farsad, A. Eckford, S. Hiyama, and Y. Moritani, "On-Chip Molecular Communication: Analysis and Design," *IEEE Transactions on NanoBioscience*, vol. 11, no. 3, pp. 304–314, 2012.

[14] M. U. Mahfuz, D. Makrakis, and H. T. Mouftah, "On the characterization of binary concentration-encoded molecular communication in nanonetworks," *Nano Communication Networks*, vol. 1, no. 4, pp. 289–300, 2010.

[15] L. C. Cobo and I. F. Akyildiz, "Bacteria-based communication in nanonetworks," *Nano Communication Networks*, vol. 1, no. 4, pp. 244–256, 2010.

[16] S. Hiyama and Y. Moritani, "Molecular communication: harnessing biochemical materials to engineer biomimetic communication systems," *Nano Communication Networks*, vol. 1, no. 1, pp. 20–30, 2010.

[17] A. W. Eckford, "Nanoscale communication with brownian motion," in *Proc. of 41st Annual Conference on Information Sciences and Systems*, (Baltimore, MD), pp. 160–165, 2007.

[18] B. Atakan and O. Akan, "An information theoretical approach for molecular communication," in *Proc. of 2nd International Conference on Bio-Inspired Models of Network, Information and Computing Systems*, (Budapest, Hungary), pp. 33–40, 2007.

[19] M. Pierobon and I. F. Akyildiz, "A physical end-to-end model for molecular communication in nanonetworks," *IEEE Journal on Selected Areas in Communications*, vol. 28, no. 4, pp. 602–611, 2010.

[20] M. Pierobon and I. Akyildiz, "Capacity of a diffusion-based molecular communication system with channel memory and molecular noise," *IEEE Transactions on Information Theory*, vol. 59, no. 2, pp. 942–954, 2013.

[21] B. Atakan and O. B. Akan, "Deterministic capacity of information flow in molecular nanonetworks," *Nano Communication Networks*, vol. 1, no. 1, pp. 31–42, 2010.

[22] T. Nakano and J.-Q. Liu, "Design and analysis of molecular relay channels: an information theoretic approach.," *IEEE Transactions on NanoBioscience*, vol. 9, pp. 213–221, Sept. 2010.

[23] M. Pierobon and I. F. Akyildiz, "Information Capacity of Diffusion-based Molecular Communication in Nanonetworks," in *Proc. of 2011 IEEE INFOCOM Workshops*, pp. 506–510, IEEE, 2011.

[24] M. Pierobon and I. F. Akyildiz, "Diffusion-based noise analysis for molecular communication in nanonetworks," *IEEE Transactions on Signal Processing*, vol. 59, no. 6, pp. 2532–2547, 2011.

[25] M. Pierobon and I. Akyildiz, "Noise analysis in ligand-binding reception for molecular communication in nanonetworks," *IEEE Transactions on Signal Processing*, vol. 59, no. 9, pp. 4168–4182, 2011.

[26] D. Miorandi, "A stochastic model for molecular communications," *Nano Communication Networks*, vol. 2, no. 4, pp. 205–212, 2011.

[27] N.-R. Kim and C.-B. Chae, "Novel Modulation Techniques Using Isomers as Messenger Molecules for Molecular Communication via Diffusion," in *Proc. of 2012 IEEE International Conference on Communications (ICC) Workshops*, (Ottawa, Canada), 2012.

[28] M. J. Moore, T. Suda, and K. Oiwa, "Molecular communication: modeling noise effects on information rate," *IEEE Transactions on NanoBioscience*, vol. 8, no. 2, pp. 169–180, 2009.

[29] N. Farsad, A. W. Eckford, S. Hiyama, and Y. Moritani, "A simple mathematical model for information rate of active transport molecular communication," in *Proc. of 2011 IEEE INFOCOM Workshops*, (Shanghai, P. R. China), pp. 473–478, 2011.

[30] N. Farsad, A. W. Eckford, and S. Hiyama, "Channel design and optimization of active transport molecular communication," in *Proc. of 6th International ICST Conference on Bio-Inspired Models of Network, Information, and Computing Systems*, (York, England), 2011.

[31] N. Farsad, A. W. Eckford, and S. Hiyama, "A mathematical channel optimization formula for active transport molecular communication," in *Proc. of 2012 IEEE International Conference on Communications (ICC) Workshops*, (Ottawa, Canada), 2012.

[32] N. Farsad, A. Eckford, and S. Hiyama, "Modelling and design of polygon-shaped kinesin substrates for molecular communication," in *Proc. of 12th IEEE Conference on Nanotechnology (IEEE-NANO)*, (Birmingham, UK), pp. 1–5, 2012.

[33] A. W. Eckford, N. Farsad, S. Hiyama, and Y. Moritani, "Microchannel molecular communication with nanoscale carriers: Brownian motion versus active transport," in *Proc. of 2010 IEEE International Conference on Nanotechnology*, (Seoul, South Korea), pp. 854 – 858, 2010.

[34] N. Farsad, A. W. Eckford, S. Hiyama, and Y. Moritani, "Information rates of active propagation in microchannel molecular communication," in *Proc. of 5th International ICST Conference on Bio-Inspired Models of Network, Information, and Computing Systems*, (Boston, MA), 2010.

[35] S. Hiyama, R. Gojo, T. Shima, S. Takeuchi, and K. Sutoh, "Biomolecular-motor-based nano- or microscale particle translocations on DNA microarrays," *Nano Letters*, vol. 9, no. 6, pp. 2407–2413, 2009.

[36] S. Hiyama, Y. Moritani, R. Gojo, S. Takeuchi, and K. Sutoh, "Biomolecular-motor-based autonomous delivery of lipid vesicles as nano- or microscale reactors on a chip," *Lab on a Chip*, vol. 10, no. 20, pp. 2741–2748, 2010.

[37] J. Howard, A. J. Hudspeth, and R. D. Vale, "Movement of microtubules by single kinesin molecules," *Nature*, vol. 342, pp. 154–158, Nov. 1989.

[38] M. G. L. van den Heuvel and C. Dekker, "Motor proteins at work for nanotechnology," *Science*, vol. 317, pp. 333–336, July 2007.

[39] T. Nitta, A. Tanahashi, M. Hirano, and H. Hess, "Simulating molecular shuttle movements: Towards computer-aided design of nanoscale transport systems," *Lab on a Chip*, vol. 6, no. 7, pp. 881–885, 2006.
[40] T. Nitta, A. Tanahashi, and M. Hirano, "In silico design and testing of guiding tracks for molecular shuttles powered by kinesin motors," *Lab on a Chip*, vol. 10, no. 11, pp. 1447–1453, 2010.
[41] T. M. Cover and J. A. Thomas, *Elements of Information Theory 2nd Edition*. Wiley-Interscience, 2 ed., 2006.
[42] R. Blahut, "Computation of channel capacity and rate-distortion functions," *IEEE Transactions on Information Theory*, vol. 18, no. 4, pp. 460–473, 1972.
[43] S. Arimoto, "An algorithm for computing the capacity of arbitrary discrete memoryless channels," *IEEE Transactions on Information Theory*, vol. 18, no. 1, pp. 14–20, 1972.
[44] MATLAB, *version 7.12.0.635 (R2011a)*. Natick, Massachusetts: The MathWorks Inc., 2011.

Nariman Farsad (S'07) received his B.Sc. and M.Sc. degrees in computer science and engineering from York University, Toronto, ON, Canada in 2007 and 2009, respectively. He is currently a Ph.D. student with the Department of Electrical Engineering and Computer Science at York University. Mr. Farsad is the recipient of Queen Elizabeth II Graduate Scholarship in Science & Technology in 2011, and the Ontario Graduate Scholarship in 2012, and 2013. He has been a Technical Reviewer for a number of journals including IEEE Transactions on Signal Processing, IEEE Transactions on Communication, and Area Associate Editor for IEEE Journal of Selected Areas of Communication–Special Issue on Emerging Technologies in Communications. He is currently interested in studying molecular and biological communication systems from both theoretical and practical perspectives.

Andrew Eckford (M'96 - S'97 - M'04) is originally from Edmonton, AB, Canada. He received the B.Eng. degree in electrical engineering from the Royal Military College of Canada, Kingston, ON, Canada, in 1996, and the M.A.Sc. and Ph.D. degrees in electrical engineering from the University of Toronto, Toronto, ON, Canada, in 1999 and 2004, respectively. He is currently an Associate Professor of Computer Science and Engineering at York University, Toronto. Dr. Eckford is also the Chair of the IEEE ComSoc Emerging Technical Subcommittee on Nanoscale, Molecular, and Quantum Networking.

Satoshi Hiyama received B.E. and M.E. degrees in Electrical Engineering from Keio University, Japan, in 1998 and 2000, respectively. He joined Network Laboratories at NTT DoCoMo, Inc., in 2000. He has been engaged in research on Quality of Service (QoS) control, call control and advanced mobility management for the Internet Protocol (IP)-based mobile networks. In mid-2003, he proposed the concept of molecular communication, which utilizes molecules as a communication medium, hoping to create a new communication paradigm based on biochemical reactions. He received a Ph.D. degree in Life Sciences from the University of Tokyo, Japan, in 2010. Dr. Hiyama organized molecular communication workshops and symposia at several biophysics conferences. He was a member of the Technical Program Committees for the BIONETICS (2006-2008, 2010, 2011), Nano-Net (2008, 2009), NanoCom (2009, 2014), MoNaCOM (2011, 2012), and ICC 2014 conferences, and currently serves on the editorial board of the Nano Communication Network (Elsevier) journal. He received the Best Paper Award for his paper presented at the International Conference on Quantum, Nano and Micro Technologies (ICQNM10), in February 2010. Currently, Dr. Hiyama is a senior research engineer at Research Laboratories, NTT DOCOMO, Inc. He is a member of the Institute of Electrical and Electronics Engineers (IEEE), the Institute of Electronics, Information and Communication Engineers (IEICE), and the Japan Society for Medical Application of Stable Isotope and Biogas. His current research interests are molecular communication and its related nanobiotechnologies.